J Solid State Electrochem (2011) 15:1845–1860
DOI 10.1007/s10008-011-1376-x

REVIEW

Solid-state electrochemical synthesis of ammonia: a review

Ibrahim A. Amar · Rong Lan · Christophe T. G. Petit · Shanwen Tao

Received: 20 January 2011 / Revised: 4 March 2011 / Accepted: 6 March 2011 / Published online: 6 April 2011

Abstract Ammonia is one of the most produced chemicals worldwide, and it is not only a major end product but also an important energy storage intermediate. The solid-state electrochemical synthesis of ammonia has the promise to overcome the limitations of the conventional catalytic reactors such as the limited conversion, severe environmental pollution and high energy consumption. Solid-state electrolytes either protonic or oxide ion conductors have been reviewed and particular emphasis is placed on their application to synthesise ammonia. The highest rate of ammonia formation according to the type of electrolyte utilised were in the following order; solid polymers > $Ce_{0.8}Gd_{0.2}O_{2-\delta}$-($Ca_3(PO_4)_2$-$K_3PO_4$) composites > fluorites > perovskites > pyrochlores although the catalysts in electrodes also play an important role. The highest rate reported so far is found to be 1.13×10^{-8} mol s^{-1} cm^{-2} at 80 °C with a potential of 2 V using Nafion membrane, $SmFe_{0.7}Cu_{0.1}Ni_{0.2}O_3$ (SFCN), and Ni-$Ce_{0.8}Sm_{0.2}O_{2-\delta}$ as solid electrolyte, cathode and anode, respectively. Synthesising ammonia from steam and N_2, by-passing H_2 stage offers many advantages such as reduction of device numbers and then the overall costs. The factors affecting the rate of ammonia formation have been discussed as well.

R. Lan · C. T. G. Petit · S. W. Tao (✉)
Department of Chemical and Process Engineering,
University of Strathclyde,
Glasgow G1 1XJ, UK
e-mail: shanwen.tao@strath.ac.uk

I. A. Amar
Department of Pure and Applied Chemistry,
University of Strathclyde,
Glasgow G1 1XL, UK

Keywords Electrochemical synthesis of ammonia · Solid-state electrolyte · Proton conductor · Oxide-ion conductor

Introduction

Ammonia (NH_3) is one of the most widely produced chemicals worldwide, and it is not only a major end product but also an important energy storage intermediate. Ammonia is a colourless alkaline gas at ambient temperature which is lighter than air and has a unique pungent, penetrating odour [1]. Ammonia and hydrogen are similar in that both could be utilised as a storage medium and clean energy carrier [2, 3].

Based on the aforementioned properties, ammonia is believed to play an important role in the world future economy. The worldwide production of ammonia is approximately 100 million tons per year. Besides, ammonia finds a widespread use in various industrial sectors including energy, refrigeration, transportation, fertilisers (more than 80% of the produced ammonia) and other industries such as pharmaceuticals and explosives production [3]. In addition, ammonia contains 17.6 wt.% hydrogen and carbon-free at the end user. Ammonia is easy to store and transport, there is an increasing interest in using ammonia as an indirect hydrogen storage material [4–6]. The energy stored in ammonia can be recovered by direct ammonia fuel cells [3, 4, 7–9].

Ammonia synthesis has a long history of developments. In 1904, the German scientist Fritz Haber started conducting a research on producing ammonia. Four years later, Haber filed his patent on the synthesis of ammonia and he was awarded the Nobel Prize in Chemistry for this invention in 1918.

Moreover, ammonia was successfully synthesised using the promoted iron-based catalyst which was discovered by Alwin Mittasch in 1910. Subsequently, Carl Bosch scaled up the ammonia synthesis process to industrial proportion for which he was awarded a Nobel Prize in 1931. Thus, today's process is known as the Haber–Bosch process: a reaction of gaseous hydrogen and nitrogen on Fe-based catalyst at high temperature (~500 °C) and high pressure (150–300 bar) [1, 10, 11].

The demand for ammonia has increased as a result of its aforementioned applications. This led to the development of alternative routes to synthesise ammonia which have the potential to overcome the limitations of the conventional catalytic reactor. Additionally, the main limitations include the low ammonia conversion, severe environmental pollution and high energy consumption [12–14]. Several synthesis approaches constitute promising alternative methods to synthesise ammonia. One of the most promising methods is the electrochemical process using either solid-state electrolytes [12, 15] or molten salts [16, 17].

To the best of our knowledge, there have been no reviews in the literature on the solid-state electrochemical synthesis of ammonia. Therefore, it is beyond the scope of writing this review to give an overview of the researches that have been conducted thus far concerning the solid-state electrochemical synthesis of ammonia. The key topics discussed include electrolytic cell component requirements, solid-state electrolyte (proton and oxide-ion conductors) with an emphasis on their application in the field of ammonia synthesis. Solid polymer electrolyte such as Nafion was also used for electrochemical synthesis of ammonia which is included in this review although polymer electrolytes are not conventional solid materials which mean solid ceramic materials. Finally, the factors that affect the rate of ammonia formation are also discussed.

Solid-state electrolytic cell component requirements

The primary components of the solid-state electrochemical device are two porous electrodes (anode and cathode) separated by a dense solid electrolyte, which allows ion transport of either protons or oxide ions and serves as a barrier to gas diffusion [18, 19]. Schematics of solid-state electrochemical ammonia synthesis devices utilising proton conducting and oxide-ion conducting electrolytes are shown in Fig. 1a and b, respectively. The general requirements for the components of the electrochemical synthesis of ammonia devices are summarised as follows [18–22];

- The electrolyte materials should exhibit high ionic conductivity in the range of 10^{-2}S cm^{-1} in order to minimise the ohmic losses, negligible electronic conductivity, mechanical strength and chemical stability in both oxidising/reducing environments.
- The solid electrolyte must be highly dense in order to be gas tight.
- Both electrodes must be stable at the operating temperature and have suitable porosity and pore size to improve the catalyst surface area and enhance the catalytic activity.
- The catalyst should possess high electronic conductivity and sufficiently high catalytic activity for ammonia synthesis.
- A good catalyst (electrode) should be a very effective hydrogen trap. By this, it is meant that the electrochemically supplied H^+ reacts on the catalyst surface to form the desired product and does not desorb to form gaseous hydrogen (H_2).
- The thermal expansion coefficients of both electrodes must be matched to that of the electrolyte to give stable interfaces and prevent material failure of the electrolyte due to the thermal expansion mismatch with other cell components.
- The cost of raw materials and fabrication should be as low as possible.

Solid-state electrolytes

Solid-state electrolytes or fast solid-state ionic conductors are an important class of materials that have received great attention because of their potential applications in gas separations, sensing of chemical species, solid oxide fuel cells, solid-state batteries, ammonia synthesis and decomposition [12, 23–26]. Recently, Garagounis et al. [27] reviewed the recent applications of the solid electrolytes in heterogeneous catalysis and chemical cogeneration. Basically, the solid electrolytes are characterised according to the conduction ions. Among these ions; proton (H^+), oxygen (O^{2-}), lithium (Li^+), copper (Cu^+), sodium (Na^+), silver (Ag^+) and fluorine (F^-) are very common [28]. Recently, Lerch et al. [29] reviewed the possibility of nitrogen ion conduction (N^{3-}) in solids such as zirconium and tantalum oxide nitrides.

In fact, Wagner [30] was the first to propose the utilisation of solid electrolytes in heterogeneous catalysis. Since then, solid-state electrolytic cells have been widely employed to study several catalytic reaction mechanisms and to provide alternative electrocatalytic routes to produce industrially important chemicals. It should be mentioned that oxygen ion conductors were used in most of the above applications [31]. Comparisons between a solid-state electrolytic reactor and a conventional heterogeneous

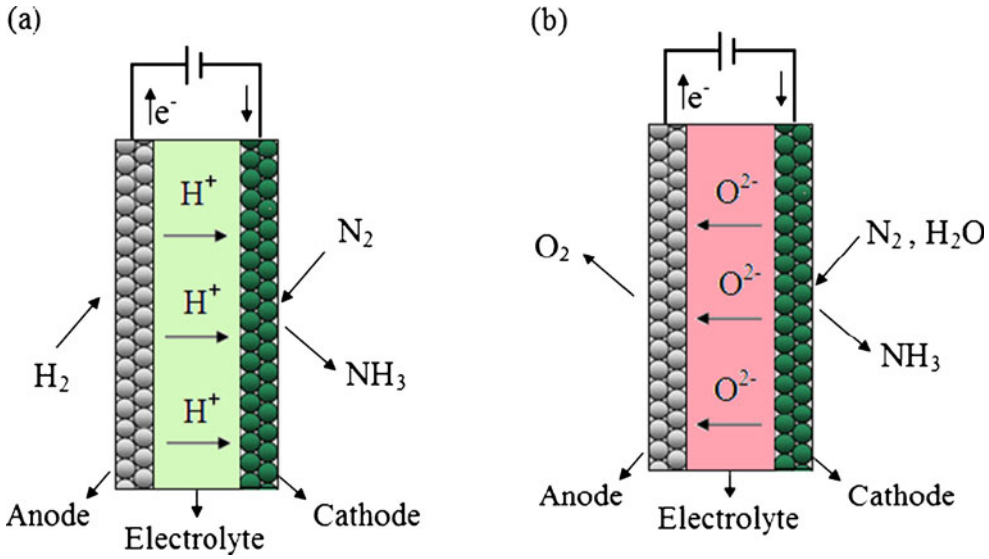

Fig. 1 Schematic illustration of solid-state electrochemical ammonia synthesis device; **a** proton-conducting electrolyte and **b** oxide-ion electrolyte

catalytic reactor have been widely made. It was found that the conversions are higher than those predicted by thermodynamic equilibrium using a solid-state electrolytic reactor. For instance, very high pressures are required for the industrially important catalytic processes namely; methanol and ammonia synthesis because the equilibrium conversion increases with increasing the total pressure. However, by using a solid-state electrolytic reactor, the requirements for high pressures are eliminated or even reversed [31–33]. The discussion below will be restricted only to solid-state proton and oxygen conductors.

Electrochemical synthesis of ammonia based on proton conducting electrolytes

Solid-state proton conductors (SSPC) represent a class of ionic solid electrolytes that have the ability to conduct hydrogen ions (H^+) [34]. It should be noted that Stotz and Wagner were the first to discuss the existence of protons in CuO, Cu_2O, NiO and in some stabilised zirconia at elevated temperature in the presence of water vapour [35]. In 1981, Iwahara et al. [36] found that some perovskites, namely strontium cerate ($SrCeO_3$) exhibited good protonic conductivity at high temperatures (600–1000 °C) in hydrogen containing atmosphere. Since then, several investigations have focused on the protonic conductivity of these materials [37–40]. According to Krug and Schober [41], the ideal proton-conducting electrolyte should possess two main features namely high hydrogen mobility and high hydrogen concentration. Kreuer [42, 43] has reviewed the proton conduction phenomena and the potential applications of the proton conductors in electrochemical devices. The proton conductivities of some solid-state electrolytes are listed in Table 1. Proton-conducting materials have found wide range of applications as electrolytes in fuel cells, solid-state batteries, hydrogen separators, steam electrolysers and ammonia synthesis and decomposition [12, 44–48]. Kreuer et al. [49] classified the solid-state proton conductors according to their operating temperature into high-, intermediate and low-temperature proton conductors. The proton conductors, rates of ammonia formation and synthesis temperatures are listed in Table 2.

In terms of preparation methods, several synthesis approaches have been employed to prepare SSPC. The conventional solid-state reaction from oxide or carbonate precursors has been widely used. However, this method suffers from some drawbacks such as high temperature requirements and formation of secondary phases [50–52]. Besides, several wet chemical methods have been utilised such as hydrothermal, co-precipitation, sol–gel process, Pechini method, citrate method and microemulsion. All these methods have the ability to reduce the sintering temperature and to provide high purity, high degree of crystallinity and good homogenous phases [53–56].

The ammonia synthesis principle

It might come as a surprise to the people who are new to the field of ammonia synthesis that the Haber–Bosch process—developed at the beginning of the twentieth century—is still the dominant process used. As previously mentioned, it involves the reaction of gaseous nitrogen and hydrogen (Eq. 3.1) on a Fe-based catalyst at high pressure (150–300 bar) and high temperature (~500 °C). The reaction is exothermic (109 kJ mol^{-1} at 500 °C) which means that the conversion increases with decreasing the operating temperature. Thus, high temperature is required to achieve industrially acceptable reaction rates. Nevertheless, major drawbacks include the fact that the conversion to ammonia (10–15%) is thermodynamically limited [12],

Table 1 The protonic conductivity of some solid electrolyte materials

Material	Proton conductivity (S cm^{-1})	Temperature (°C)	References
Perovskite-type			
$SrCe_{0.95}Yb_{0.05}O_{3-\delta}$ (SCY)	0.05×10^{-2}–1.8×10^{-2}	800–1000	[54]
$SrZr_{0.95}Y_{0.05}O_{3-\delta}$ (SZY)	3.05×10^{-3}–2.1×10^{-2}	600–1000	[59]
$BaCe_{0.85}Y_{0.15}O_{3-\delta}$ (BCY)	1.04×10^{-2}	600	[66]
$BaCe_{0.85}Sm_{0.15}O_{3-\delta}$ (BCS)	4.75×10^{-2}–7.78×10^{-2}	800–900	[40]
$La_{0.9}Sr_{0.1}Ga_{0.8}Mg_{0.2}O_{3-\delta}$ (LSGM)	1.4×10^{-2}	520	[79]
$La_{0.9}Ca_{0.1}Ga_{0.8}Mg_{0.2}O_{3-\delta}$ (LCGM)	0.42×10^{-2}	520	[79]
$La_{0.9}Ba_{0.1}Ga_{0.8}Mg_{0.2}O_{3-\delta}$ (LBGM)	0.82×10^{-2}	520	[79]
$BaCe_{0.85}Gd_{0.15}O_{3-\alpha}$ (BCGO)	1.4×10^{-2}	600	[64]
$Ba_3(Ca_{1.18}Nb_{1.82})O_{9-\delta}$ (BCN18)	1.3×10^{-2}	600	[80]
$BaCe_{0.9}Ca_{0.1}O_{3-\delta}$ (BCC)	7.64×10^{-4}	600	[118]
$BaCe_{0.85}Dy_{0.15}O_{3-\delta}$ (BCD)	0.93×10^{-2}	600	[61]
Pyrochlore-type			
$La_{1.95}Ca_{0.05}Zr_2O_{7-\delta}$ (LCZ)	6.8×10^{-2}	600	[47]
Fluorite-type			
$Ce_{0.8}La_{0.2}O_{2-\delta}$ (LDC)	1.9×10^{-2}	650	[97]
$Ce_{0.8}Y_{0.2}O_{2-\delta}$ (YDC)	2.3×10^{-2}	650	[97]
$Ce_{0.8}Gd_{0.2}O_{2-\delta}$ (GDC)	2.6×10^{-2}	650	[97]
$Ce_{0.8}Sm_{0.2}O_{2-\delta}$ (SDC)	3.8×10^{-2}	650	[97]
$(Ce_{0.8}La_{0.2})_{0.975}Ca_{0.025}O_{3-\delta}$ (CLC)	5.9×10^{-2}	800	[98]
Polymer-type			
Nafion	5×10^{-2}–4×10^{-2}	25–160	[47]

environmental pollution is severe and energy consumption is high [13, 14].

$$N_2 + 3H_2 \leftrightarrow 2NH_3 \tag{3.1}$$

Panagos et al. [32] proposed a model process using solid-state proton conductor to overcome the thermodynamic constraints of the reversible reaction (3.1). The principle is explained in Fig. 1a and Fig. 2 using either H_2 or steam (H_2O), respectively. In the electrolytic cell, two metal electrodes are placed on both sides of the proton conductor. The gaseous H_2 passing over the anode will be converted to H^+ (Eq. 3.2). Hydrogen in the form of protons will be transported to the cathode where the half-cell reaction (Eq. 3.3) will take place; hence Eq. 3.1 is the overall reaction.

$$6H \rightarrow 6H^+ + 6e^- \tag{3.2}$$

$$N_2 + 6H^+ + 6e^- \rightarrow 2NH_3 \tag{3.3}$$

Recently, Skodra and Stoukides [57] proposed another ammonia synthesis principle using steam rather than molecular H_2 (Fig. 2). The H_2O passing over the anode will be converted to H^+ and O_2:

$$3H_2O \rightarrow 6H^+ + \frac{3}{2}O_2 + 6e^- \tag{3.4}$$

Then the protons will be transported through the electrolyte to the cathode where the half-cell reaction (Eq. 3.3) takes place

Hence the overall reaction is:

$$3H_2O + N_2 \rightarrow 2NH_3 + \frac{3}{2}O_2 \tag{3.5}$$

Perovskite-type oxides

The perovskite-type oxides have the typical formula ABO_3, in which the A-site is occupied by a large 12-coordinated cation typically a rare earth and the B-site is occupied by a small six-coordinated cation (BO_6octahedra) frequently a transition metal [58]. Figure 3 represents the typical perovskite structure of barium cerate-based oxides ($BaCeO_3$). Many zirconate and cerate perovskite oxides namely $CaZrO_3$, strontium zirconate ($SrZrO_3$) or $SrCeO_3$ show reasonable proton conductivity at elevated temperatures and under hydrogen-containing atmosphere. Additionally, their formula could be written as $AB_{1-x}M_xO_{3-\delta}$ in which *M* is a trivalent cation such as Y^{3+}, Gd^{3+}, Yb^{3+}, Nd^{3+}, Sm^{3+} etc. or divalent cation such as Ca^{2+} and δ the oxygen deficiency in the oxide lattice [47, 59, 60].

$SrCeO_3$-based electrolytes As reported by Iwahara et al. [36], $SrCeO_3$-based oxides were the first class of perovskites

Table 2 Summary of the SSPC electrolytes and the rates of ammonia formation

Proton Conductor	Electrolytic Cell	Temperature (°C)	NH_3 Formation rate (mol s^{-1} cm^{-2})	References
Perovskite-type				
SCY	H_2, Pd |SCY| Pd, N_2, NH_3, He	570	4.5×10^{-9}	[12]
SCY	H_2, Pd |SCY| Pd, N_2, NH_3, He	570	1.6×10^{-9}	[44]
SCY	Steam H_2O, Pd |SCY| Ru-based catalyst, N_2, NH_3	650	9.1×10^{-14}	[57]
BCN18	H_2, Ag–Pd |BCN18| Ag–Pd, N_2, NH_3	620	1.42×10^{-9}	[55]
BCZN	H_2, Ag–Pd |BCZN| Ag–Pd, N_2, NH_3	620	1.82×10^{-9}	[55]
BCNN	H_2, Ag–Pd |BCNN| Ag–Pd, N_2, NH_3	620	2.16×10^{-9}	[55]
BCS	H_2, Ag–Pd |BCS| Ag–Pd, N_2, NH_3	620	5.23×10^{-9}	[65]
BCGS	H_2, Ag–Pd |BCGS| Ag–Pd, N_2, NH_3	620	5.82×10^{-9}	[65]
LSGM	H_2, Ag–Pd |LSGM| Ag–Pd, N_2, NH_3	550	3.37×10^{-9}	[53]
LCGM	H_2, Ag–Pd |LCGM| Ag–Pd, N_2, NH_3	520	$1.6\ 3\times10^{-9}$	[79]
LSGM	H_2, Ag–Pd |LSGM| Ag–Pd, N_2, NH_3	520	2.53×10^{-9}	[79]
LBGM	H_2, Ag–Pd |LBGM| Ag–Pd, N_2, NH_3	520	2.04×10^{-9}	[79]
LBGM	H_2, Ag–Pd |LBGM| Ag–Pd, N_2, NH_3	520	1.89×10^{-9}	[78]
BCGO	H_2, Ni-BCGO |BCGO| Ag–Pd, N_2, NH_3	480	4.63×10^{-9}	[64]
SZY	H_2, Ag |SZY| Fe catalyst, N_2, NH_3	450	6.2×10^{-12}	[76]
BCGO	H_2, Ag–Pd |BCGO| Ag–Pd, N_2, NH_3	480	3.09×10^{-9}	[63]
BCY	H_2, Ag–Pd |BCY| Ag–Pd, N_2, NH_3	500	2.1×10^{-9}	[66]
BCY	H_2, Ni-BCY |BCY| BSCF, N_2, NH_3	530	4.1×10^{-9}	[67]
BCD	H_2, Ag–Pd |BCD| Ag–Pd, N_2, NH_3	530	3.5×10^{-9}	[61]
BCC	H_2, Ag–Pd |BCC| Ag–Pd, N_2, NH_3	480	2.69×10^{-9}	[68]
Pyrochlore-type				
LCZ	H_2, Ag–Pd |LCZ| Ag–Pd, N_2, NH_3	520	2.0×10^{-9}	[54]
LCC	H_2, Ag–Pd |LCC| Ag–Pd, N_2, NH_3	520	1.3×10^{-9}	[87]
LCZO	H_2, Ag–Pd |LCZO| Ag–Pd, N_2, NH_3	520	2.0×10^{-9}	[87]
Fluorite-type				
LDC	H_2, Ag–Pd |LDC| Ag–Pd, N_2, NH_3	650	7.2×10^{-9}	[97]
YDC	H_2, Ag–Pd |YDC| Ag–Pd, N_2, NH_3	650	7.5×10^{-9}	[97]
GDC	H_2, Ag–Pd |GDC| Ag–Pd, N_2, NH_3	650	7.7×10^{-9}	[97]
SDC	H_2, Ag–Pd |SDC| Ag–Pd, N_2, NH_3	650	8.2×10^{-9}	[97]
LDC	H_2, Ag–Pd | LDC| Ag–Pd, N_2, N H_3	650	7.2×10^{-9}	[98]
CLC	H_2, Ag–Pd |CLC| Ag–Pd,N_2, NH_3	650	7.5×10^{-9}	[98]
YDC	H_2, Ag–Pd |YDC| Ag–Pd, N_2, NH_3	650	6.5×10^{-9}	[111]
Polymer-type				
Nafion	H_2O, Pt |Nafion| Ru, N_2, NH_3	90	2.12×10^{-11}	[99]
Nafion	H_2, Ni-SDC |Nafion| SFCN, N_2, NH_3	80	1.13×10^{-8}	[101]
SPSF	H_2, Ni-SDC |Nafion| SSCO, N_2, NH_3	80	6.5×10^{-9}	[100]
Nafion	H_2, Ni-SDC |Nafion| SSN, N_2, NH_3	80	1.05×10^{-8}	[14]
Nafion	H_2, Ni-SDC |Nafion| SSC, N_2, NH_3	80	0.98×10^{-8}	[14]
Nafion	H_2, Ni-SDC |Nafion| SSF, N_2, NH_3	80	0.92×10^{-8}	[14]
Nafion	H_2, Ni-SDC |Nafion| SSN, N_2, NH_3	80	1.05×10^{-8}	[13]
SPSF	H_2, Ni-SDC | SPSF | SSN, N_2, NH_3	80	1.03×10^{-8}	[13]
Nafion	H_2, Ni-SDC |Nafion| SBCF, N_2, NH_3	80	7.0×10^{-9}	[102]
Nafion	H_2, Ni-SDC |Nafion| SBCC, N_2, NH_3	80	7.5×10^{-9}	[102]
Nafion	H_2, Ni-SDC |Nafion| SBCN, N_2, NH_3	80	8.7×10^{-9}	[102]
Composite electrolytes				
YDC-($Ca_3(PO_4)_2$-K_3PO_4)	H_2, Ag–Pd | YDC-($Ca_3(PO_4)_2$-K_3PO_4)| Ag–Pd, N_2, NH_3	650	9.5×10^{-9}	[111]

Table 2 (continued)

Proton Conductor	Electrolytic Cell	Temperature (°C)	NH_3 Formation rate ($mols^{-1}$ cm^{-2})	References
YDC-($Ca_3(PO_4)_2$-K_3PO_4)	Natural gas, Ag–Pd |YDC-($Ca_3(PO_4)_2$-K_3PO_4)| Ag–Pd, N_2, NH_3	650	6.95×10^{-9}	[112]
Carbonate-$LiAlO_2$	H_2, Ag–Pd |Carbonate-$LiAlO_2$| CFO-Ag, N_2, NH_3	400	2.32×10^{-10}	[114]

SCY $SrCe_{0.95}Yb_{0.05}O_{3-\delta}$, *LCZ* $La_{1.9}Ca_{0.1}Zr_2O_{6.95}$, *BCN18* $Ba_3(Ca_{1.18}Nb_{1.82})O_{9-\delta}$, *BCZN* $Ba_3CaZr_{0.5}Nb_{1.5}O_{9-\delta}$, *BCNN* $Ba_3Ca_{0.9}Nd_{0.28}Nb_{1.82}O_{9-\delta}$, *LCC* $La_{1.95}Ca_{0.05}Ce_2O_{7-\delta}$, *LCZO* $La_{1.95}Ca_{0.05}Zr_2O_{7-\delta}$, *LDC* $Ce_{0.8}La_{0.2}O_{2-\delta}$, *YDC* $Ce_{0.8}Y_{0.2}O_{2-\delta}$, *GDC* $Ce_{0.8}Gd_{0.2}O_{2-\delta}$, *SDC* $Ce_{0.8}Sm_{0.2}O_{2-\delta}$, *BCS* $BaCe_{0.9}Sm_{0.1}O_{3-\delta}$, *BCGS* $BaCe_{0.8}Gd_{0.1}Sm_{0.1}O_{3-\delta}$, *LSGM* $La_{0.9}Sr_{0.1}Ga_{0.8}Mg_{0.2}O_{3-\delta}$, *SFCN* $SmFe_{0.7}Cu_{0.1}Ni_{0.2}O_3$, *BCGO* $BaCe_{0.85}Gd_{0.15}O_{3-\delta}$, *SZY* $SrZr_{0.95}Y_{0.05}O_{3-\delta}$, *BCY* $BaCe_{0.85}Y_{0.15}O_{3-\delta}$, *BCD* $BaCe_{0.85}Dy_{0.15}O_{3-\delta}$, *BCC* $BaCe_{0.9}Ca_{0.1}O_{3-\delta}$, *LDC* $Ce_{0.8}La_{0.2}O_{3-\delta}$, *CLC* $(Ce_{0.8}La_{0.2})_{0.975}$-$Ca_{0.025}O_{3-\delta}$, *YDC* $Ce_{0.8}Y_{0.2}O_{1.9}$, *SSCO* $Sm_{0.5}Sr_{0.5}CoO_{3-\delta}$, *SSC* $Sm_{1.5}Sr_{0.5}CoO_4$, *SSN* $Sm_{1.5}Sr_{0.5}NiO_4$, *SSF* $Sm_{1.5}Sr_{0.5}FeO_4$, *LCGM* $La_{0.9}Ca_{0.1}Ga_{0.8}Mg_{0.2}O_{3-\delta}$, *LBGM* $La_{0.9}Ba_{0.1}Ga_{0.8}Mg_{0.2}O_{3-\delta}$, *SPSF* sulfonated polysulfone, *SBCF* $SmBaCuFeO_{5+\delta}$, *SBCC* $SmBaCuCoO_{5+\delta}$, *SBCN* $SmBaCuNiO_{5+\delta}$, *BSCF* $Ba_{0.5}Sr_{0.5}Co_{0.8}Fe_{0.2}O_{3-\delta}$, *CFO* $CoFe_2O_4$

that exhibit protonic conductivity under hydrogen containing atmosphere and elevated temperatures. The basic formula of doped strontium cerates can be written as follows $SrCe_{1-x}M_xO_{3-\delta}$in which M is an aliovalent cation such as Yb^{3+}, Sc^{3+}, Y^{3+}, etc.

Based on the model proposed by Panagos et al. [32], Marnellos and Stoukides [12] in 1998 reported an alternative route to synthesise ammonia from its elements (H_2 and N_2) at atmospheric pressure for the first time using the solid-state proton conductor strontia-ceria-ytterbia (SCY) in the form of $SrCe_{0.95}Yb_{0.05}O_3$ as an electrolyte and palladium (Pd) as the electrodes. In addition, greater than 78% of the supplied protons were converted into ammonia. Two years later, Marnellos et al. [15, 44] used the aforementioned conditions to synthesise ammonia using two different reactors (double- and single-chamber cells) and it was found that nearly 80% of the electrochemically supplied hydrogen was converted into ammonia at 570–750 °C and atmospheric pressure. More recently, Skodra and Stoukides [57] reported the synthesis of ammonia for the first time from nitrogen and steam rather than molecular hydrogen. It is worth stressing that using steam instead of hydrogen is advantageous in that the costs of both the production and further purification of hydrogen will be eliminated. At the anode, steam is electrolysed to H^+ and O_2 (Eq. 3.5) and only H^+ will be transported through the solid electrolyte to the cathode where it reacts with the adsorbed nitrogen to produce ammonia (Eq. 3.3). This means that only nitrogen needs purification and pure oxygen can be produced at minimal cost. The ammonia was synthesised successfully in electrolytic cell at 450–700 °C using SCY, Ru-based catalyst, and Pd as solid electrolyte, cathode and anode, respectively. However, the

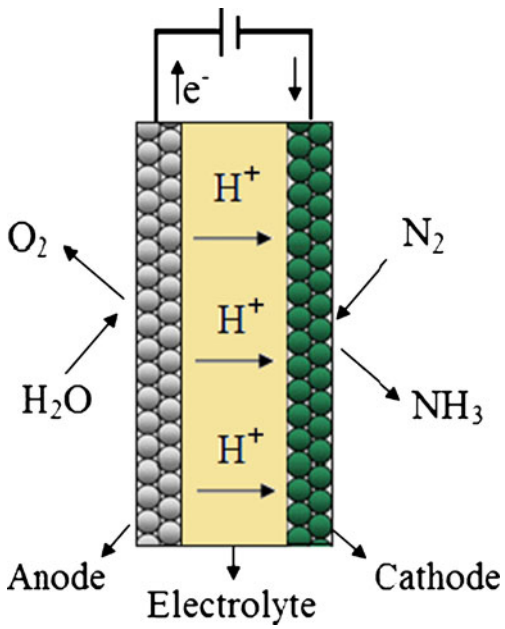

Fig. 2 Schematic diagram of the ammonia synthesis device using H_2O and N_2

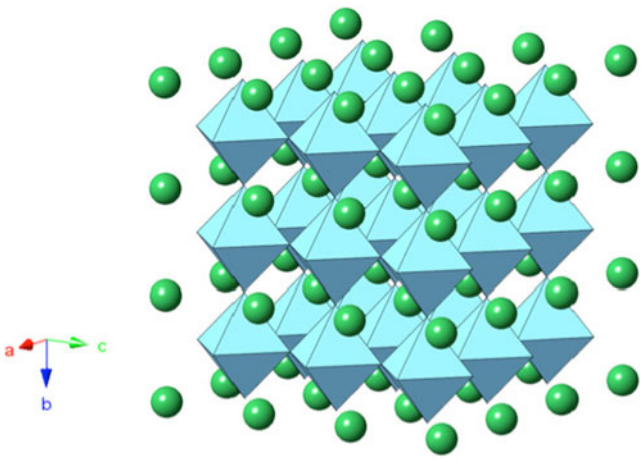

Fig. 3 The perovskite $BaCeO_3$ structure, the spheres represent the barium atoms

conversion of either nitrogen or steam into ammonia was low, primarily due to the difficulty of imposing high proton fluxes through the electrolytic cell and the poor electrical conductivity of the working electrode.

$BaCeO_3$-based electrolytes $BaCeO_3$ are one of the most studied proton conducting materials. Doped barium cerates $BaCe_{1-x}M_xO_{3-\delta}$ in which M is a trivalent cation such as Y^{3+}, Gd^{3+}, Yb^{3+}, Nd^{3+}, Dy^{3+} or Sm^{3+} are considered as good candidate as proton conducting materials for solid oxide fuel cells (SOFC) [40, 57, 61]. In addition, these materials exhibit higher proton conductivity than zirconate oxides such as $SrZrO_3$ [62]. However, below around 800 °C, these oxides are not stable in air and lose the protonic conduction because they easily react with carbon dioxide to form alkaline earth carbonates [50].

Gd-doped barium cerate (BCGO) in the form of $BaCe_{0.8}Gd_{0.2}O_{3-\delta}$ was prepared via the citrate method and used as a solid electrolyte to synthesise ammonia. Ag–Pd was utilised as electrodes and the rate of ammonia formation was up to 3.09×10^{-9} mol s^{-1} cm^{-2} at 480 °C [63]. Chen et al. [64] reported the use of the microemulsion method to prepare gadolinium-doped $BaCeO_3$ owing to its advantage in reducing the sintering temperature, the formation of high purity phases and the homogeneity of the components. Ammonia was synthesised in an electrolytic cell based on BCGO in the form of $BaCe_{0.85}Gd_{0.15}O_{3-\delta}$ as a solid electrolyte and Ni-BCGO and Ag–Pd were used as anode and cathode, respectively. The rate of ammonia formation was then 4.63×10^{-9} mol s^{-1} cm^{-2} at 480 °C. Li et al. [65] employed the sol–gel process to prepare the single and double-doped $BaCeO_3$ oxides in form of $BaCe_{0.9}Sm_{0.1}O_{3-\delta}$ (BCS) and $BaCe_{0.8}Gd_{0.1}Sm_{0.1}O_{3-\delta}$ (BCGS), respectively. BCS and BCGS were used as solid electrolytes and Ag–Pd as electrodes. Ammonia was synthesised at atmospheric pressure and the rates of ammonia formation were found to be up to 5.23×10^{-9} and 5.82×10^{-9} mol s^{-1} cm^{-2} for BCS and BCGS, respectively, at 620 °C.

Y-doped $BaCeO_3$ (BCY) in the form of $BaCe_{0.85}Y_{0.15}O_{3-\delta}$ has been prepared by the microemulsion method and successfully applied as a solid electrolyte to synthesise ammonia at atmospheric pressure. Ag–Pd alloy was used as electrodes and the rate of ammonia formation was 2.1×10^{-9} mol s^{-1} cm^{-2}at 500 °C with an applied current of 0.75 mA [66]. Recently, Wang et al. [67] successfully assembled a tri-layer membrane reactor for ammonia synthesis at atmospheric pressure comprised of a thin electrolyte membrane (~30 μm) ($BaCe_{0.85}Y_{0.15}O_{3-\delta}$, BCY) and two electrode layers (Ni-BCY anode substrate and $Ba_{0.5}Sr_{0.5}Co_{0.8}Fe_{0.2}O_{3-\delta}$ (BSCF) cathode). Ammonia was successfully synthesised from H_2 and N_2 in a membrane electrolytic reactor and the maximum rate of ammonia formation 4.1×10^{-9} mol s^{-1} cm^{-2} at 530 °C was obtained with an imposed DC current of 1 mA. The results indicated that the rate of ammonia formation was higher than that of $BaCe_{0.85}Y_{0.15}O_{3-\delta}$ (thickness ~ 0.8 mm) [66].

Dy-doped $BaCeO_3$ in form of $BaCe_{0.85}Dy_{0.15}O_{3-\delta}$ was synthesised by the means of microemulsion process and employed for ammonia synthesis at atmospheric pressure and intermediate temperature. Ag–Pd was used as electrodes and ammonia was successfully synthesised from wet H_2 and dry N_2 at a rate of 3.5×10^{-9} mol s^{-1} cm^{-2} at 530 °C with an imposed current of 1.2 mA. In addition, the results confirmed that Dy-doped $BaCeO_3$ electrolyte has excellent proton conduction at an intermediate temperature (300–600 °C) and it could be utilised as an alternative proton conductor for application at this temperature range [61].

Ca-doped $BaCeO_3$ (BCC) exhibits lower proton conductivity compared to rare earth metals oxide-doped $BaCeO_3$. However, due to the rich source and cheapness of calcium oxide, Ca-doped $BaCeO_3$ is still interesting [68]. Iwahara et al. [60] reported that $BaCe_{1-x}Ca_xO_{3-\delta}$ exhibits both protonic and oxide ionic conduction at high temperatures (600–1,000 °C). Liu et al. [68] investigated the protonic conductivity of BCC at intermediate temperature in the range of 300–600 °C and its application in ammonia synthesis. BCC in the form of $BaCe_{1.9}Ca_{0.1}O_{3-\delta}$ was synthesised by microemulsion route and utilised as solid electrolyte and Ag–Pd as electrodes to synthesise ammonia from wet H_2 and dry N_2 under atmospheric pressure. The maximum rate of ammonia formation and the current efficiency of the electrochemically supplied H_2 were 2.69×10^{-9} mol s^{-1} $cm^{-2}$and about 50%, respectively, with an applied current of 0.8 mA at 480 °C.

$CaZrO_3$-based electrolytes In general, alkaline earth zirconate oxides such as $CaZrO_3$, $SrZrO_3$ and $BaZrO_3$ exhibit extremely high chemical stability and are stronger—mechanically speaking—compared to alkaline earth cerate oxides [50, 62, 69–71]. Moreover, in-doped $CaZrO_3$ (CZI) is regarded as the most suitable proton conductor for practical use at high temperature owing to its chemical stability and mechanical strength, despite the fact that its proton conduction is lower than that of cerate based oxides [62, 72–74].

Yiokari et al. [75] utilised in-doped $CaZrO_3$ in the form of $CaZr_{0.9}In_{0.1}O_{3-\delta}$, a commercial Fe-based catalyst and Ag as solid electrolyte, cathode and anode, respectively, to synthesise ammonia under high pressure (50 bar) at 440 °C. In that study, it was found that the rate of ammonia formation could be enhanced by up to 1,300% by interfacing the catalyst with the proton conductor and supplying the protons to the catalyst electrochemically via application of a potential (typically −1 V) between the working electrode and the silver reference electrode. Wherein, the effect of electrochemical promotion or non-

Faradaic electrochemical modification of catalytic activity was first demonstrated under high pressure (50 bar).

$SrZrO_3$-based electrolytes As mentioned above, $SrZrO_3$-based oxides are one of the alkaline earth zirconate which exhibit extremely high chemical stability. In addition, $SrZrO_3$ shows protonic conduction at high temperatures when it is doped with some trivalent cations such as In^{3+}, Sc^{3+}, Y^{3+}, etc. This means that it is suitable for practical use at high temperature in steam electrolysis, in fuel cells and for hydrogen gas sensors [55].

Ouzounidou et al. [76] investigated the synthesis of ammonia in both single-chamber and double-chamber reactor cells. Y-doped $SrZrO_3$ in the form of $SrZr_{0.95}Y_{0.05}O_{3-\delta}$, an industrial Fe-based catalyst and Ag were employed as solid electrolyte, working electrode and anode, respectively. Ammonia was successfully synthesised under atmospheric pressure and temperature in the range of 450–700 °C with nearly 80% conversion.

$LaGaO_3$-based electrolytes Lanthanum gallate ($LaGaO_3$)-based oxides possess a higher ionic conductivity in comparison to yttria-stabilised zirconia (YSZ)-based oxides and thus regarded as promising electrolytes for electrochemical cells operating at intermediate temperature (500–800 °C). Ma et al. [77] were the first to discover the proton conduction in Sr and Mg-doped $LaGaO_3$ in form of $La_{0.9}Sr_{0.1}Ga_{0.8}Mg_{0.2}O_{3-\delta}$.

Zhang et al. [53] were the first to synthesise $La_{0.9}Sr_{0.1}Ga_{0.8}Mg_{0.2}O_{3-\delta}$ via the microemulsion method and applied it to synthesise ammonia at atmospheric pressure with a rate of ammonia formation in the cathode chamber of 2.37×10^{-9} mol s^{-1} cm^{-2} at 550 °C. Chen et al. [78] synthesised $La_{0.9}Ba_{0.1}Ga_{0.8}Mg_{0.2}O_{3-\delta}$ via the microemulsion method and employed it as solid electrolyte to synthesise ammonia from wet hydrogen and dry nitrogen under atmospheric pressure. Ag–Pd was used as electrodes (cathode and anode) and the rate of ammonia formation was found to be 1.89×10^{-9} mol s^{-1} cm^{-2} at 520 °C upon imposing a current of 1 mA through the electrolytic cell. Recently, Cheng et al. [79] have prepared $La_{0.9}M_{0.1}Ga_{0.8}Mg_{0.2}O_{3-\delta}$ (M=Ca^{2+}, Sr^{2+}, Ba^{2+}) via a hydrothermal precipitation method and applied them as solid electrolyte to synthesise ammonia. Ag–Pd was used as electrodes and the rates of ammonia formation were found to be 1.63×10^{-9}, 2.53×10^{-9} and 2.04×10^{-9} mol s^{-1} $cm^{-2}$when M=Ca^{2+}, Sr^{2+} and Ba^{2+}, respectively, at 520 °C.

Complex perovskite-type oxides Complex perovskite-type oxides represent another type of high-temperature proton conductors (HTPC). They are nonstoichiometric or mixed perovskites of $A_3(B'B_2'')O_9$ type in which A ions are always bi-charged cations such as alkaline earth elements (Ca, Sr, Ba, etc.) while B′ is either 2+or 3+and B″ is 5+. Furthermore, their formula can be written as $A_3B'_{1+X}B''_{2-X}O_9$ [41, 52, 80–85]. Li et al. [55] employed the citrate method to prepare ultra-fine powders of $B_3(Ca_{1.18}Nb_{1.82})O_{9-\delta}$ (BCN18), $Ba_3Ca_{0.9}Nd_{0.28}Nb_{1.82}O_{9-\delta}$ (BCNN), and $Ba_3CaZr_{0.5}Nb_{1.5}O_{9-\delta}$ (BCZN). Ammonia was synthesised at atmospheric pressure using BCN18, BCZN, and BCNN as solid electrolytes and Ag–Pd as electrodes. The maximum rates of ammonia formation were as follows; 1.42×10^{-9}, 1.82×10^{-9}, and 2.16×10^{-9} mol s^{-1} cm^{-2} at 620 °C for BCN18, BCZN, and BCNN, respectively.

Pyrochlore-type oxides

In addition to the perovskite-type electrolytes, non-perovskite oxides including; pyrochlores, fluorites, phosphates and sulphates, exhibit protonic conduction at elevated temperatures under hydrogen-containing atmosphere [86].

Pyrochlore-type oxides have the general formula $A_2B_2O_7$ with two types of cations (A^{3+} and B^{4+}) as shown in Fig. 4. Pyrochlores can be regarded as (A, B)O_2 fluorite structures depending on the cation radius ratio: when $r^{3+}/r^{4+}>1.22$ it is considered as a pyrochlore ($La_2Zr_2O_7$) while it is a fluorite structure otherwise ($La_2Ce_2O_7$). Furthermore, at high temperature—generally as high as 1,377–2,227 °C—most pyrochlores disorder into fluorite structure [87–89]. Generally, these materials have attracted great attention as fast ionic conductors because of the presence of many non-occupied sites [90–92]. Shimura et al. [93] reported proton conduction in lanthanum zirconate-based oxides ($La_2Zr_2O_7$) at high temperature and under hydrogen-containing atmosphere.

Ca-doped $La_2Zr_2O_7$ (LCZ) in the form of $La_{1.9}Ca_{0.1}Zr_2O_{6.95}$ has been prepared by sol–gel process and used as a solid electrolyte and Ag–Pd as electrodes.

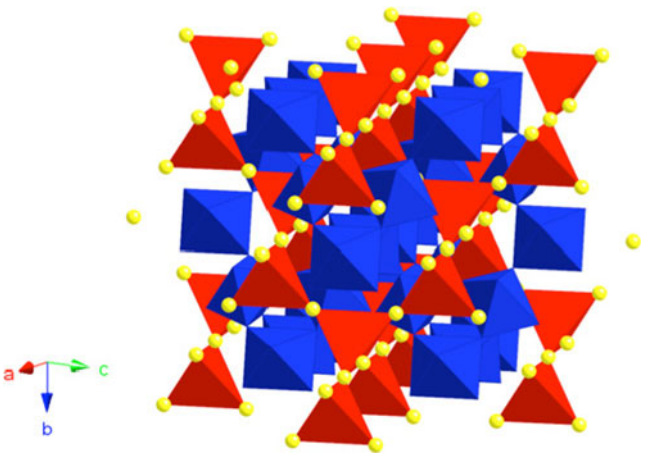

Fig. 4 The pyrochlore $La_2Zr_2O_7$ structure, the spheres represent the zirconium atoms

Ammonia was successfully synthesised from H_2 and N_2 at atmospheric pressure and the rate of ammonia formation was up to 2.0×10^{-9} mol s^{-1} cm^{-2} with more than 80% of the electrochemically supplied hydrogen converted into ammonia at 520 °C [54]. Wang et al. [87] employed complex oxides such as $La_{1.95}Ca_{0.05}Ce_2O_{7-\delta}$ (LCC) and $La_{1.95}Ca_{0.05}Zr_2O_{7-\delta}$ as solid electrolytes that were prepared by the sol–gel method to synthesise ammonia. It was found that the rates of ammonia were up to 2.0×10^{-9} and 1.3×10^{-9} mol s^{-1} cm^{-2} for LCZ and LCC, respectively, at 520 °C.

Fluorite-type oxides

The fluorite-type oxides are considered as the traditional oxygen ion-conducting electrolytes. The fluorite oxide has the general formula AO_2 in which A is a large tetravalent cation and is presented in Fig. 5. Examples of materials that easily adopt the fluorite structure are ceria (CeO_2), uranium dioxide and thorium dioxide [58].

It is worth bearing in mind that the protonic conductivity of these materials has been overlooked for a long time; however, Nigara et al. [94] in 1998 was the first to suggest a possibility of protonic conductivity. Since then, several subsequent researches have been conducted to confirm this possibility [94–96]. Moreover, according to Liu et al. [97], the protonic conductivity of doped-CeO_2 electrolytes would lead to lower the cell efficiency and fuel permeation which is not desirable for SOFC. However, it is a valuable property for hydrogen production, hydrogen sensors and the electrochemical synthesis of ammonia.

Rare earth-doped CeO_2 in the form of La-doped ceria (LDC), Y-doped (YDC), Gd-doped ceria (GDC) and Sm-doped ceria (SDC) has been prepared via the sol–gel process. With $Ce_{0.8}M_{0.2}O_{2-\delta}$ (*M*=La, Y, Gd, Sm) as solid electrolyte and Ag–Pd as electrodes, ammonia was successfully synthesised at atmospheric pressure and intermediate temperature. The ammonia formation rates were 7.2×10^{-9}, 7.5×10^{-9}, 7.7×10^{-9} and 8.2×10^{-9} mol s^{-1} cm^{-2} for LDC, YDC, GDC and SDC, respectively, at 650 °C [97]. Liu et al. [98] employed rare earth-doped CeO_2 oxides in the form of $Ce_{0.8}La_{0.2}O_{3-\delta}$ (LDC) and $(Ce_{0.8}La_{0.2})_{0.975}Ca_{0.025}O_{3-\delta}$ (CLC) which were prepared by a sol–gel process as solid electrolytes and Ag–Pd as electrodes. The maximum rates of ammonia formation were 7.2×10^{-9} and 7.5×10^{-9} mol s^{-1} cm^{-2} at 650 °C for LDC and CLC, respectively. Consequently, one could conclude that the rates of ammonia formation of doped-CeO_2 exceeded that for pyrochlore-based and perovskite-type oxides.

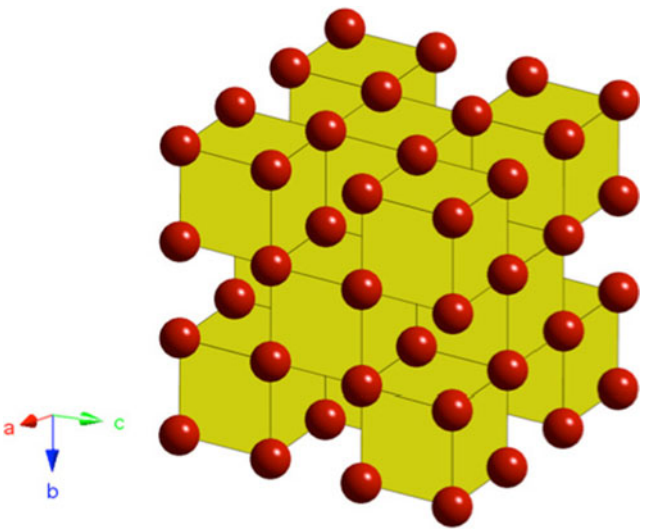

Fig. 5 The fluorite CeO_2 structure, the spheres represent the oxygen atoms

Polymer-type electrolyte

As mentioned in the preceding sections, ammonia was synthesised at atmospheric pressure with the use of HTPC. However, relatively high temperatures are required at which ammonia decomposition occurs and thus limits the yield of ammonia. Hence, Kordali et al. [99] utilised a solid polymer electrolyte cell to synthesise ammonia at low temperature and atmospheric pressure. Ammonia was successfully synthesised from nitrogen and water at 90 °C using Nafion as a solid electrolyte and ruthenium as an electrode. Nevertheless, the rate of ammonia formation was quite low (2.12×10^{-11} mol s^{-1} cm^{-2}) which was attributed to the nature of the Ru catalyst. Wang et al. [100] successfully demonstrated the synthesis of ammonia by using a sulfonated polysulfone (SPSF) proton exchange membrane, SSCO in the form of $Sm_{0.5}Sr_{0.5}CoO_{3-\delta}$ and NiO-$Ce_{0.8}Sm_{0.2}O_{2-\delta}$ (Ni-SDC) as solid electrolyte, cathode and anode, respectively. The rate of ammonia was found to be up to 6.5×10^{-9} mol s^{-1} cm^{-2} at 80 °C under atmospheric pressure. Xu et al. [101] reported the synthesis of ammonia from its elements (N_2 and H_2) at atmospheric pressure and low temperatures from 25 to 100 °C. SFCN in the form of $SmFe_{0.7}Cu_{0.1}Ni_{0.2}O_3$, Nafion membrane, and nickel-samaria-doped ceria in the form of Ni-SDC were used as cathode, solid electrolyte, and anode, respectively. The highest rate of ammonia formation obtained using $SmFe_{0.7}Cu_{0.1}Ni_{0.2}O_3$ as a cathode was 1.13×10^{-8} mol s^{-1} cm^{-2} at 80 °C with a potential of 2 V. It is worth bearing in mind that this is the highest rate of ammonia production reported in the literature so far. Furthermore, the current efficiency when Nafion was used as a solid electrolyte to synthesise ammonia reached as high as 90.4% which is higher than that obtained with HTPC materials. Xu et al. [14] synthesised ammonia using Nafion as electrolyte and Ni-SDC as anode. In that study, three types of cathode catalysts were prepared by the sol–gel method in the form of $Sm_{1.5}Sr_{0.5}MO_4$ (*M*=Ni, Co, Fe) and it was found that the

highest rate of ammonia was up to 1.05×10^{-8} mol s^{-1} cm^{-2} at 80 °C and 2.5 V when $Sm_{1.5}Sr_{0.5}NiO_4$ (SSN) was used. Recently, Liu et al. [13] has reported the synthesis of ammonia using SPSF and Nafion membranes as electrolytes where SSN and Ni-SDC were utilised as cathode and anode, respectively. Despite the fact that the Nafion membrane possesses higher protonic conductivity than SPSF, the ammonia formation rates are almost the same 1.03×10^{-8} and 1.05×10^{-8} mol s^{-1} cm^{-2} at 80 °C under atmospheric pressure. This means that the Nafion membrane could be completely replaced by the SPSF membrane in the electrochemical synthesis of ammonia. More recently, Zhang et al. [102] reported the synthesis of ammonia using a Nafion proton exchange membrane, $SmBaCuMO_{5+\delta}$ (M=Fe, Co, Ni) which was prepared via the citrate sol–gel method and Ni-SDC as electrolyte, cathode and anode, respectively. The cathode catalysis performance of $SmBaCuMO_{5+\delta}$ (M= Fe, Co, Ni) for ammonia synthesis was investigated with wet hydrogen and dry nitrogen under atmospheric pressure. The rates of ammonia formation were 7.0×10^{-9}, 7.5×10^{-9} and 8.7×10^{-9} mol s^{-1} cm^{-2} for $SmBaCuFeO_{5+\delta}$, $SmBaCuCoO_{5+\delta}$ and $SmBaCuNiO_{5+\delta}$, respectively, at 80 °C with an applied potential of 2.5 V. Consequently, it may be concluded that Nafion and SPSF membranes are more efficient than HTPC and can be utilised in the electrochemical synthesis of ammonia at low temperature.

Composite electrolytes

Composite electrolytes represent a mixture of two or more phases with different properties such as enhanced ionic or thermal conductivities and mechanical properties [103]. In recent years, ceria-salt composite materials have drawn considerable interest owing to their potential applications as electrolytes for intermediate temperature solid oxide fuel cells and hydrogen sensors. These materials consist of two-phases, ceria-based oxide as a host phase and second salt phase such as carbonates, halides, sulphates or hydrates [104–110]. Wang et al. [111] prepared a series of a new type of oxide-salt composite electrolyte by mixing the yttrium doped ceria (YDC, $Ce_{0.8}M_{0.2}O_{1.9}$) which was synthesised via sol–gel method and binary phosphates ($Ca_3(PO_4)_2$-K_3PO_4) according to different weight ratios. Ammonia was successfully synthesised from nitrogen and hydrogen at atmospheric pressure using YDC-($Ca_3(PO_4)_2$-K_3PO_4) composite and Ag–Pd alloy as solid electrolyte and electrodes, respectively. The rates of ammonia formation were found to be up to 6.5×10^{-9}, 5.8×10^{-9}, 9.5×10^{-9} and 7.8×10^{-9} mol s^{-1} cm^{-2} for pure YDC, YDC-30 wt.% ($Ca_3(PO_4)_2$-K_3PO_4), YDC-20 wt.% ($Ca_3(PO_4)_2$-K_3PO_4), YDC-10 wt.% ($Ca_3(PO_4)_2$-K_3PO_4), respectively, at 650 °C and with an applied potential of 0.6 V. The results indicated that the protonic conductivity of YDC was improved by adding the binary phosphates which in turn resulted in a higher ammonia formation rate. In addition, the optimal composite electrolyte composition was 80 wt.% YDC-20 wt.% binary phosphate ($Ca_3(PO_4)_2$-K_3PO_4).

It should be stressed that the most conducted researches on ammonia synthesis have focused on using H_2 and N_2. Wang et al. [112] was the first to synthesise ammonia from N_2 and natural gases (methane or ethane) rather than molecular hydrogen in solid-state proton conductor cells at atmospheric pressure and intermediate temperature. Oxide-salt composite electrolyte YDC-($Ca_3(PO_4)_2$-K_3PO_4) prepared by mixing of 80 wt.% YDC with 20 wt.% binary phosphate ($Ca_3(PO_4)_2$-K_3PO_4) was applied to the synthesis of ammonia. The rate of ammonia was up to 6.95×10^{-9} mol s^{-1} cm^{-2} at 650 °C with an applied potential of 1.0 V. According to these results, ammonia was successfully synthesised with the use of solid-state proton conductor from nitrogen and direct use of natural gas. The possible ammonia synthesis mechanism (Fig. 6) is as follows:

$$2CH_4 \rightarrow C_2H_6 + H_2 \tag{3.6}$$

$$2CH_4 \rightarrow C_2H_4 + 2H_2 \tag{3.7}$$

$$C_2H_6 \rightarrow C_2H_4 + H_2 \tag{3.8}$$

As can be seen from Fig. 6, the natural gases (methane or ethane) can be converted to hydrogen with the use of the oxide-salt composite electrolyte YDC-($Ca_3(PO_4)_2$-K_3PO_4) and the ammonia was synthesised from nitrogen and hydrogen according to Eqs. 3.2 and 3.3.

Non-ceria-based composite electrolytes have been investigated as candidate electrolytes for fuel cell applications. Li et al. [113] employed a novel non-ceria-based composites a solid electrolyte for low or intermediate temperature fuel cells. Recently, we have reported the synthesis of ammonia for the first time using non-ceria composite electrolyte based on carbonate-$LiAlO_2$and $CoFe_2O_4$ spinel catalyst. The rate of ammonia was found to be up to 2.32×10^{-10} mol s^{-1} s^{-1} cm^{-2} at 400 °C with an applied potential of 0.8 V [114].

Electrochemical synthesis of ammonia based on oxygen ion conducting electrolytes

In addition to the proton-conducting electrolytes, oxygen-conducting ceramics can be used to synthesise ammonia at atmospheric pressure. Ionic solid electrolytes which conduct only oxygen ions (O^{2-}) are known as oxide-ion electrolytes [115]. Recently, Skodra and Stoukides [57] reported the synthesis of ammonia for the first time in an electrolytic cell at 450–700 °C using the oxygen ion conductor YSZ,

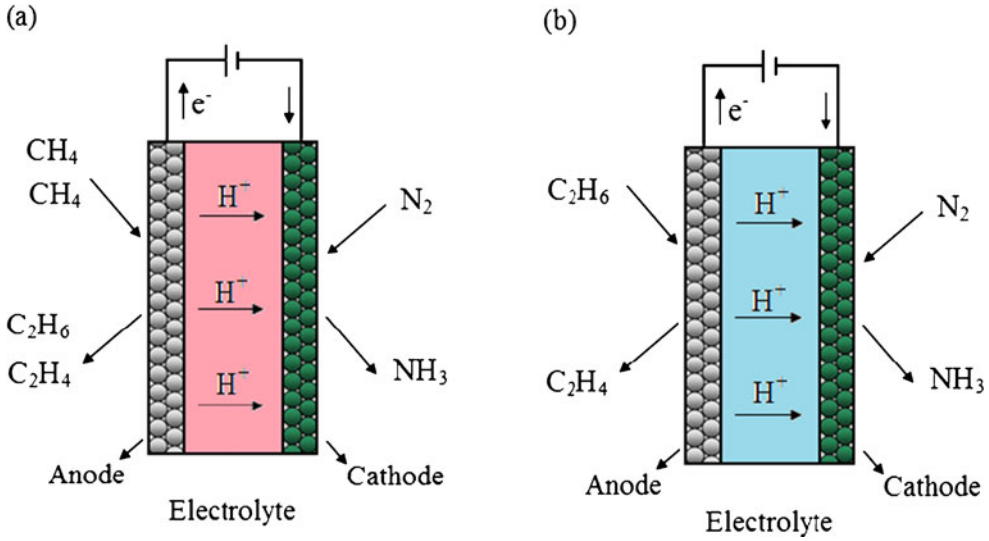

Fig. 6 Ammonia synthesis principle using natural gases and nitrogen

Ru-based catalyst, and Pd as solid electrolyte, cathode, and anode, respectively. Furthermore, ammonia was also synthesised from nitrogen and water steam rather than molecular hydrogen. It is worth bearing in mind that the conversion of either nitrogen or steam to ammonia was low which might be due to the poor electric conductivity of the working electrode (Ru-based catalyst). Additionally, the principle of the electrochemical synthesis of ammonia using oxide-ion conductors can be written as follows (Fig. 1b):

Cathode reaction:

$$3H_2O + N_2 + 6e^- \rightarrow 3O^{2-} + 2NH_3 \quad (3.9)$$

Anode reaction:

$$3O^{2-} \rightarrow \frac{3}{2}O_2 + 6e^- \quad (3.10)$$

The overall reaction is the same as in Eq. 3.6.

Factors affecting the rate of ammonia formation

The catalytic reaction of the synthesis of ammonia has been studied intensively in heterogeneous catalysis because of its industrial and economic importance. It is worth noting that the electrocatalytic synthesis of ammonia using solid-state proton conductors at atmospheric pressure was first investigated by Marnellos et al. [12, 15, 44]. Moreover, it has been found that the reaction rate could be enhanced by pumping H^+ to the catalyst surface. Also, nearly 80% of the electrochemically supplied hydrogen was convertible into ammonia.

The key parameters affecting the rate of ammonia formation are quite complex including; volumetric flow rates of N_2 and H_2, electrode materials, area of electrode, electrical conductivity of the working electrode (catalyst), electrode polarisation, synthesis temperature, employed potential, applied current, the rate of ammonia decomposition, the ammonia synthesis reactor configuration, electrolyte materials and thickness of electrolyte [53, 57, 64, 67]. It should be noticed that the reaction rate also depends on other experimental conditions such as N_2 partial pressure and proton flux. The reaction rate is still listed in Table 2 for reference although they may be obtained under different conditions.

Effect of the applied current

Guo et al. [66] investigated the influence of the applied current on the rate of ammonia production at the synthesis temperature of 500 °C. No NH_3 was synthesised when the current (I) was equal to 0 mA. Upon imposing a current through the cell, the rate of ammonia formation increased significantly with increasing the applied current up to 0.75 mA; however, by further increasing the applied current, the rate of ammonia formation remained almost the same as illustrated in Fig. 7. However, Wang et al. [67] observed a different trend, the rate of the ammonia formation increased with increasing the applied current up to 1 mA and then declined significantly after 1 mA which could be attributed to nitrogen chemisorption hindered by the high rate of electrochemically supplied H^+, which in turn poisoned the catalyst (cathode surface) as illustrated in Fig. 8.

Effects of cathode catalyst materials and conductivity

Xu and Liu [14] investigated the effect of the working electrode (catalyst) materials on the rate of ammonia formation. Basically, three different electrodes—SSN, $Sm_{1.5}Sr_{0.5}CoO_4$ (SSC) and $Sm_{1.5}Sr_{0.5}FeO_4$ (SSF)—were compared and it was found that SSN was a better cathode

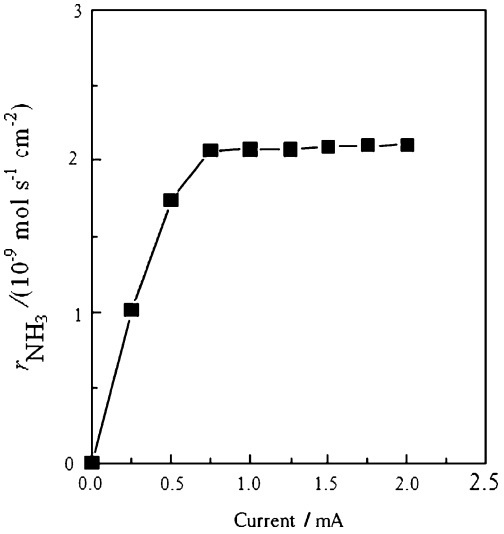

Fig. 7 Dependence of the ammonia formation rate on the applied current. The electrolytic cell was: wet H_2, Ag–Pd |BCY| Ag–Pd, dry N_2 and at operating temperature 500 °C [66]

catalyst in ammonia synthesis than SSC and SSF (Table 2). Besides, one of the main obstacles to obtain high ammonia formation rate is the poor electrical conductivity of the working electrode (catalyst) [67]. Skodra and Stoukides [57] investigated the electrocatalytic synthesis of ammonia using Ru-based industrial catalyst as a working electrode. The results indicated that the ammonia formation rate was rather low which was attributed to the poor electric conductivity of Ru-based catalyst despite the fact that it is very active for ammonia synthesis. To overcome this problem, a thin Ag layer was deposited on the solid electrolyte and then the active catalyst was added on the top of the metal layer. However, a significant fraction of the H^+ combined on the Ag film to form gaseous H_2 and never reached the catalyst surface. Ouzounidou et al. [76] demonstrated the electrocatalytic synthesis of ammonia using an industrial Fe-based catalyst (modified Fe_3O_4) in which the active phase is oxidic not metallic. However, unlike metals, oxides exhibit much lower electronic conductivities. The solution adopted was to prepare the electrode by depositing a thin metal (Fe) layer on the electrolyte and then the oxide catalyst was added on the top. Nevertheless, protons reacted with nitrogen on the Fe metal layer when they reached the metal-electrolyte-gas boundary at the cathode, and the metallic phase is a poor catalyst for ammonia synthesis. Thus, catalyst-electrode design is of crucial importance to improve the rate of ammonia formation.

Besides the electronic conductivity and the catalytic activity of the working electrode, the electrode polarisation may play a major role on the rate of ammonia formation. Wang et al. [67] employed BSCF which exhibits good mixed electronic–ionic conduction properties as a working electrode for ammonia synthesis. However, the ammonia formation rate was rather low which was ascribed to the high electrode polarisation.

Effect of the imposed potential

The effects played by the imposed potential on the rate of ammonia formation have also been widely investigated [53, 55, 63, 87, 97]. According to Li et al. [63], the ammonia production rate is potential dependent. As can be seen in Fig. 9, no ammonia was produced when the potential was equal to 0 V. However, the ammonia formation rate increased with increasing the imposed potential up to 0.6 V and remained almost constant by further increasing the

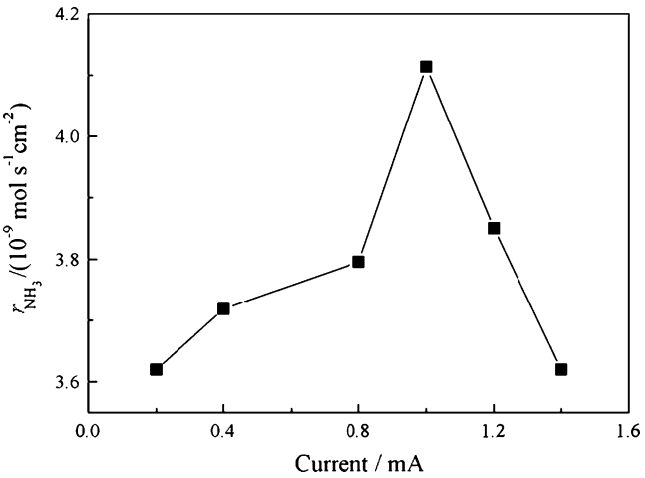

Fig. 8 Dependence of the ammonia formation rate on the applied current. The electrolytic cell was: wet H_2, Ni-BCY |BCY| BSCF, dry N_2 and the operating temperature 530 °C [67]

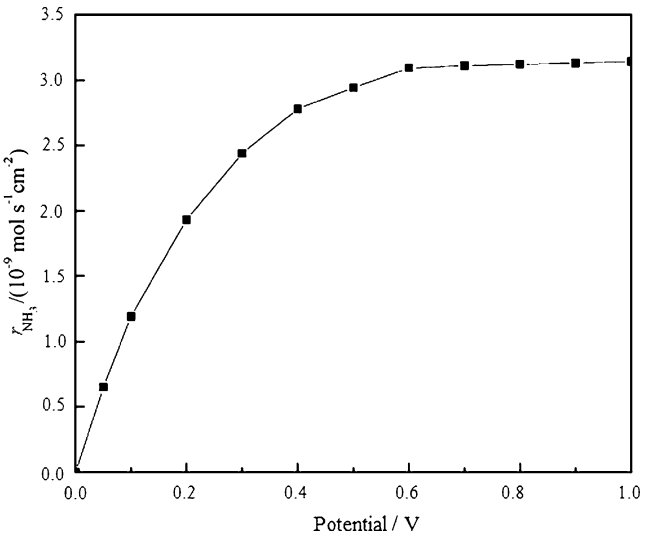

Fig. 9 Effect of imposed potential on the ammonia formation rate. The electrolytic cell was: H_2, Ag–Pd |BCGO| Ag–Pd, N_2 and the operating temperature 480 °C [63]

potential up to 1.0 V. It is worth mentioning that the catalyst surface area of the electrode employed in that study was 1.13 cm^2 which is not sufficient to convert all electrochemically supplied H_2 into NH_3. Li et al. [55] and Zhang et al. [53] stated that in order to increase the H_2 conversion rate into NH_3, it is necessary to; increase the electrode surface area and catalyst, find new efficient catalysts for NH_3 formation and prepare a thin film of electrolyte.

Effect of operating temperature

In terms of the impacts of operating temperature on the rate of ammonia production, Chen and Ma [64] demonstrated that the ammonia formation rate increases as the operating temperature is increased from 400 to 480 °C which could be attributed to the increase of protonic conductivity in the utilised electrolyte ($BaCe_{0.85}Gd_{0.15}O_{3-\delta}$). However, a rate-degrading tendency was obtained when the operating temperature was further increased up to 560 °C which certainly results from the ammonia decomposition as shown in Fig. 10. This also explains the peak observed in the rate of NH_3 formation as a function of the operating temperature. Hence, the electrolytic cell configuration (design) is important to diminish the rate of ammonia decomposition [12].

The influence of operating temperature on the rate of ammonia formation has also been investigated at low temperature (25–100 °C). Liu et al. [13] utilised solid polymer membranes (Nafion and SPSF) as solid electrolytes and studied the effect of operating temperature on the ammonia production rate. Their results are in good agreement with the aforementioned study in which high temperature proton conductors are used as a solid electrolyte. The rate of ammonia formation increased remarkably with increasing of operating temperature as illustrated in Fig. 11. However, the ammonia production rate decreased significantly with further increasing the operating temperature which was ascribed to the decrease of proton conductivity due to water loss. The ammonia decomposition does not play important role on the ammonia formation rate since the operating temperature was quite low.

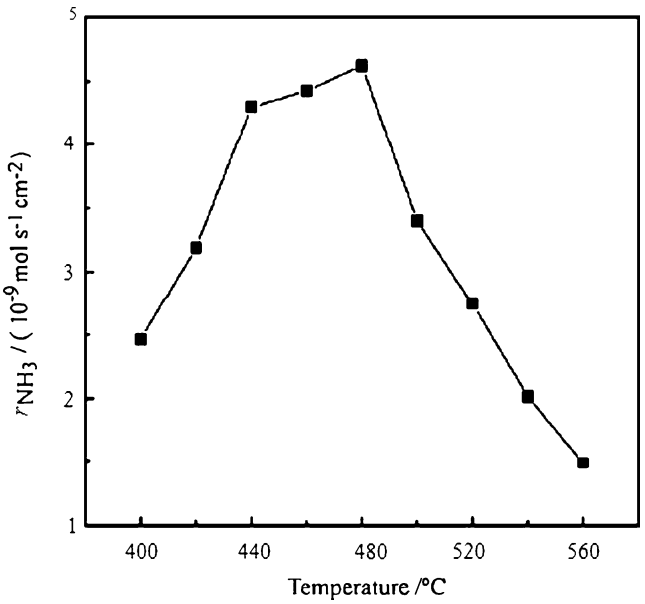

Fig. 10 The relationship between the rate of ammonia formation and the synthesis temperature. The cell was H_2, Ni-BCGO |BCGO| Ag–Pd, N_2 [64]

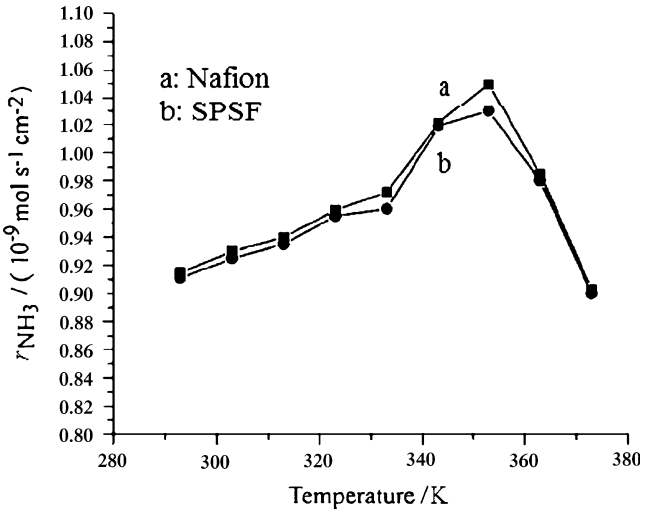

Fig. 11 Dependence of ammonia formation rate on the operating temperature when polymers used as electrolytes. The electrolytic cells were (*a*) wet H_2, Ni-SDC |Nafion| SSN, dry N_2; (*b*) wet H_2, Ni-SDC | SPSF| SSN, dry N_2 [13]

Effects of electrolyte materials and thickness

The electrolyte materials and thickness also play an important role on the rate of ammonia formation. In general, as summarised in Table 2, by using different electrolyte materials, the ammonia formation rate varied significantly. Furthermore, the highest rate of ammonia formation according to the type of electrolyte utilised were in the following order; solid polymers > YDC-phosphate composites > fluorites > perovskites > pyrochlores. Wang et al. [111] investigated the effect of the electrolyte materials on the ammonia formation rate by adding binary phosphates to the YDC in the form of $Ce_{0.8}M_{0.2}O_{1.9}$ according to different weight ratios to prepare oxide solid composite YDC-($Ca_3(PO_4)_2$-K_3PO_4). It was found that the rate of ammonia production increased by adding the binary phosphates which could be attributed to the increase in the protonic conductivity of the solid electrolyte composite.

As mentioned above, the thickness of the electrolyte is one of the crucial factors that affect the rate of ammonia formation. By reducing the thickness of the electrolyte layer, the operating temperature could be lowered which is beneficial to improve the ammonia-formation rate. It is

desirable to operate the electrochemical devices at an intermediate temperature, because of the significant advantages such as lower manufacturing costs, more flexible choice of materials and longer lifetime [61]. It is well known that the ionic conductivity of the electrolytes decreases significantly with decreasing the operating temperature which in turn results in high Ohmic losses across the electrolyte. The Ohmic losses can be overcome or minimised by either reducing the electrolyte thickness or with employing materials of high ionic conductivity at low temperature [116, 117]. Guo et al. [66] reported the synthesis of ammonia at an intermediate temperature using $BaCe_{0.85}Y_{0.15}O_{3-\delta}$ (thickness, ~ 0.8 mm) as solid electrolyte and maximum rate of ammonia evolution was up to 2.1×10^{-9} mol s^{-1} cm^{-2}at 500 °C. More recently, Wang et al. [67] successfully prepared a dense, thin proton conducting membrane ($BaCe_{0.85}Y_{0.15}O_{3-\delta}$) with a thickness about 0.03 mm. The thin electrolyte employed to synthesise ammonia had a maximum rate of 4.1×10^{-9} mol s^{-1} cm^{-2}at 530 °C. The results revealed that by reducing the thickness of the electrolyte from 0.8 to 0.03 mm the ammonia formation rate almost doubled and the current efficiency of membrane reactor improved obviously.

Conclusions

This review has highlighted the solid-state electrochemical synthesis of ammonia technology. Solid-state proton conductors such as perovskites, pyrochlores, fluorites and polymers have been reviewed and discussed in detail with particular emphasis on their application in ammonia synthesis. The ammonia synthesis using oxide-ion electrolyte has also been presented. The rates of ammonia formation and the employed proton conductors have been listed in Table 2 and the highest rate was found to be 1.13×10^{-8} mol s^{-1} cm^{-2} at 80 °C with a potential of 2 V using Nafion, $SmFe_{0.7}Cu_{0.1}Ni_{0.2}O_3$, and Ni-SDC as solid electrolyte, cathode and anode, respectively. The factors affecting the rate of ammonia formation have been discussed as well.

Synthesising ammonia from N_2 and steam instead of molecular H_2 using either proton or oxide-ion conducting electrolytes may offer many advantages as the electrolyser for hydrogen production is not required.

In conclusion, there has been considerable progress made in the development of solid-state electrochemical synthesis of ammonia technology to improve the rate of ammonia formation. However, in order to make a breakthrough in the field of solid-state ammonia synthesis, to increase ammonia formation rate, continuing efforts to discover novel compounds are needed. This means exploring new electrolyte materials that provide high ionic conductivity at low temperature, effective cathode and anode materials of high electronic conductivity and catalytic activity for ammonia synthesis. Combined with direct ammonia fuel cells, this technology has the potential to be used for energy storage.

Acknowledgement The authors gratefully thank EPSRC for funding. One of the authors (Ibrahim A. Amar) thanks The Libyan Cultural Affairs, London for the financial support of his study in the UK.

References

1. Slack A, James G (1973) Ammonia part I. Fertilisers science and technology series-, vol 2. Marcel Dekker, Inc, New York
2. Douglas J (1971) Synthesis of ammonia, Englishth edn. The Macmillan Press Ltd., New York
3. Zamfirescu C, Dincer I (2008) J Power Sources 185:459–465
4. Lan R, Tao SW (2010) Electrochem Solid-State Lett 13:B83–B86
5. Green L Jr (1982) An ammonia energy vector for the hydrogen economy. Int J Hydrogen Energy 7(4):355–359
6. Klerke A, Christensen CH, Nørskov JK, Vegge T (2008) Ammonia for hydrogen storage: challenges and opportunities. J Mater Chem 18(20):2304–2310
7. Zamfirescu C, Dincer I (2009) Fuel Process Technol 90:729–737
8. Alagharu V, Palanki S, West KN (2010) J Power Sources 195:829–833
9. Zhang L, Yang W (2008) J Power Sources 179:92–95
10. Appl M (1997) The Haber–Bosch heritage: the ammonia production technology. 50th Anniversary of the IFA Technical Conference September 25–26th 1997, Sevilla, Spain
11. Erisman J, Sutton M, Galloway J, Klimont Z, Winiwarter W (2008) Nat Geosci 1:636–639
12. Marnellos G, Stoukides M (1998) Science 282:98–100
13. Liu R, Xu G (2010) Chin J Chem 28:139–142
14. Xu G, Liu R (2009) Chin J Chem 27:677–680
15. Marnellos G, Karagiannakis G, Zisekas S, Stoukides M (2000) Stud Surf Sci Catal 130:413–418
16. Murakami T, Nishikiori T, Nohira T, Ito Y (2003) J Am Chem Soc 125:334–335
17. Murakami T, Nohira T, Goto T, Ogata Y, Ito Y (2005) Electrochim Acta 50:5423–5426
18. Malavasi L, Fisher CAJ, Islam MS (2010) Chem Soc Rev 39:4370–4387
19. Tillement O (1994) Solid State Ionics 68:9–33
20. Ni M, Leung MKH, Leung DYC (2008) Int J Hydrogen Energy 33:2337–2354
21. Jacobson A (2010) Chem Mater 22:660–674
22. Marnellos G, Athanasiou C, Tsiakaras P, Stoukides M (1996) Ionics 2:412–420
23. Liu M, Khandkar A (1992) Solid State Ionics 52:3–13
24. Hong Y (1997) J Mater Sci Technol 13:173–178
25. Mazanec T (1994) Solid State Ionics 70:11–19
26. Zisekas S, Karagiannakis G, Kokkofitis C, Stoukides M (2008) J Appl Electrochem 38:1143–1149
27. Garagounis I, Kyriakou V, Anagnostou C, Bourganis V, Papachristou I, Stoukides M (2011) Ind Eng Chem Res 50:431–472
28. Stoukides M (1988) Ind Eng Chem Res 27:1745–1750
29. Lerch M, Janek J, Becker KD, Berendts S, Boysen H, Bredow T, Dronskowski R, Ebbinghaus SG, Kilo M, Lumey MW (2009) Progr Solid State Chem 37:81–131
30. Wagner C (1970) Adv Catal 21:323–381

31. Marnellos G, Sanopoulou O, Rizou A, Stoukides M (1997) Solid State Ionics 97:375–383
32. Panagos E, Voudouris I, Stoukides M (1996) Chem Eng Sci 51:3175–3180
33. Marnellos G, Kyriakou A, Florou F, Angelidis T, Stoukides M (1999) Solid State Ionics 125:279–284
34. Norby T (1999) Solid State Ionics 125:1–11
35. Stotz S, Wagner C (1966) Ber Bunsenges Phys Chem 70:781–788
36. Iwahara H, Esaka T, Uchida H, Maeda N (1981) Solid State Ionics 3:359–363
37. Slade R, Singh N (1993) Solid State Ionics 61:111–114
38. Iwahara H (1992) Solid State Ionics 52:99–104
39. Chiodelli G, Malavasi L, Tealdi C, Barison S, Battagliarin M, Doubova L, Fabrizio M, Mortal C, Gerbasi R (2009) J Alloys and Com 470:477–485
40. Gorbova E, Maragou V, Medvedev D, Demin A, Tsiakaras P (2008) J Power Sources 181:207–213
41. Krug F, Schober T (1996) Solid State Ionics 92:297–302
42. Kreuer KD (1996) Chem Mater 8:610–641
43. Kreuer K (2003) Annu Rev Mater Res 33:333–359
44. Marnellos G, Zisekas S, Stoukides M (2000) J Catal 193:80–87
45. Kokkofitis C, Ouzounidou M, Skodra A, Stoukides M (2007) Solid State Ionics 178:507–513
46. Iwahara H, Uchida H, Tanaka S (1986) J Appl Electrochem 16:663–668
47. Phair J, Badwal SPS (2006) Ionics 12:103–115
48. Skodra A, Ouzounidou M, Stoukides M (2006) Solid State Ionics 177:2217–2220
49. Kreuer K (1997) Solid State Ionics 97:1–15
50. Iwahara H, Yajima T, Hibino T, Ozaki K, Suzuki H (1993) Solid State Ionics 61:65–69
51. Zhai Y, Ye C, Xiao J, Dai L (2006) J Power Sources 163:316–322
52. Nowick A, Du Y, Liang K (1999) Solid State Ionics 125:303–311
53. Zhang F, Yang Q, Pan B, Xu R, Wang H, Ma G (2007) Mater Lett 61:4144–4148
54. Xie YH, Wang JD, Liu RQ, Su XT, Sun ZP, Li ZJ (2004) Solid State Ionics 168:117–121
55. Li ZJ, Liu RQ, Xie YH, Feng S, Wang JD (2005) Solid State Ionics 176:1063–1066
56. Eschenbaum J, Rosenberger J, Hempelmann R, Nagengast D, Weidinger A (1995) Solid State Ionics 77:222–225
57. Skodra A, Stoukides M (2009) Solid State Ionics 180:1332–1336
58. Skinner SJ, Kilner JA (2003) Mater Today 6:30–37
59. Hibino T, Mizutani K, Yajima T, Iwahara H (1992) Solid State Ionics 57:303–306
60. Iwahara H, Mori T, Hibino T (1995) Solid State Ionics 79:177–182
61. Wang W, Liu J, Li Y, Wang H, Zhang F, Ma G (2010) Solid State Ionics 181:667–671
62. Tanaka M, Ohshima T (2010) Fusion Eng Des 85:1038–1043
63. Li ZJ, Liu RQ, Wang JD, Xie YH, Yue F (2005) J Solid State Electrochem 9:201–204
64. Chen C, Ma G (2009) J Alloys Comp 485:69–72
65. Li ZJ, Liu RQ, Wang JD, Xu Z, Xie YH, Wang BH (2007) Sci Technol Adv Mater 8:566–570
66. Guo Y, Liu B, Yang Q, Chen C, Wang W, Ma G (2009) Electrochem Commun 11:153–156
67. Wang W, Cao X, Gao W, Zhang F, Wang H, Ma G (2010) J Membr Sci 360:397–403
68. Liu J, Li Y, Wang W, Wang H, Zhang F, Ma G (2010) J Mater Sci 45:5860–5864
69. Le J, Van Rij L, Van Landschoot R, Schoonman J (1999) J Eur Ceram Soc 19:2589–2591
70. Zhou M, Ahmad A (2008) Sens Actuators B: Chem 129:285–291
71. Dudek M (2009) Mater Res Bull 44:1879–1888
72. Fukatsu N, Kurita N, Yajima T, Koide K, Ohashi T (1995) J Alloys Comp 231:706–712
73. Shi C, Yoshino M, Morinaga M (2005) Solid State Ionics 176:1091–1096
74. Higuchi T, Yamaguchi S, Kobayashi K, Shin S, Tsukamoto T (2003) Solid State Ionics 162:121–125
75. Yiokari C, Pitselis G, Polydoros D, Katsaounis A, Vayenas C (2000) J Phys Chem A 104:10600–10602
76. Ouzounidou M, Skodra A, Kokkofitis C, Stoukides M (2007) Solid State Ionics 178:153–159
77. Ma G, Zhang F, Zhu J, Meng G (2006) Chem Mater 18:6006–6011
78. Chen C, Ma G (2008) J Mater Sci 43:5109–5114
79. Cheng C, Wenbao W, Guilin M (2009) Acta Chim Sin 67:623–628
80. Du Y, Nowick A (1996) Solid State Ionics 91:85–91
81. Nowick A, Du Y (1995) Solid State Ionics 77:137–146
82. Schober T, Friedrich J, Triefenbach D, Tietz F (1997) Solid State Ionics 100:173–181
83. Bohn H, Schober T, Mono T, Schilling W (1999) Solid State Ionics 117:219–228
84. Schober T, Bohn H, Mono T, Schilling W (1999) Solid State Ionics 118:173–178
85. Tao SW, Irvine JTS (2002) Solid State Ionics 154:659–667
86. Shimura T, Fujimoto S, Iwahara H (2001) Solid State Ionics 143:117–123
87. Wang JD, Xie YH, Zhang ZF, Liu RQ, Li ZJ (2005) Mater Res Bull 40:1294–1302
88. Kutty K, Mathews C, Rao T, Varadaraju U (1995) Solid State Ionics 80:99–110
89. Kharton V, Marques F, Atkinson A (2004) Solid State Ionics 174:135–149
90. Wilde P, Catlow C (1998) Solid State Ionics 112:173–183
91. Wuensch BJ, Eberman KW, Heremans C, Ku EM, Onnerud P, Yeo EME, Haile SM, Stalick JK, Jorgensen JD (2000) Solid State Ionics 129:111–133
92. Isasi J, Lopez M, Veiga M, Pico C (1996) Solid State Ionics 89:321–326
93. Shimura T, Komori M, Iwahara H (1996) Solid State Ionics 86:685–689
94. Nigara Y, Mizusaki J, Kawamura K, Kawada T, Ishigame M (1998) Solid State Ionics 113:347–354
95. Sakai N, Yamaji K, Horita T, Yokokawa H, Hirata Y, Sameshima S, Nigara Y, Mizusaki J (1999) Solid State Ionics 125:325–331
96. Nigara Y, Yashiro K, Kawada T, Mizusaki J (2001) Solid State Ionics 145:365–370
97. Liu RQ, Xie YH, Wang JD, Li ZJ, Wang BH (2006) Solid State Ionics 177:73–76
98. Liu RQ, Xie YH, Li ZJ, Wang JD (2005) YG S. Acta Phys Chim Sin 21:967–970
99. Kordali V, Kyriacou G, Lambrou C (2000) Chem Commun 31 (48):1673–1674
100. Wang J, Liu RQ (2008) Acta Chim Sin 66:717–721
101. Xu GC, Liu RQ, Wang J (2009) Sci China Ser B: Chem 52:1171–1175
102. Zhang Z, Zhong Z, Liu R (2010) J Rare Earths 28:556–559
103. Schober T (2005) Electrochem Solid-State Lett 8:A199
104. Zhu B, Liu X, Zhou P, Zhu Z, Zhu W, Zhou S (2001) J Mater Sci Lett 20:591–594
105. Zhu B (2003) J Power Sources 114:1–9
106. Di J, Chen M, Wang C, Zheng J, Fan L, Zhu B (2010) J Power Sources 195:4695–4699
107. Zhu B, Yang X, Xu J, Zhu Z, Ji S, Sun M, Sun J (2003) J Power Sources 118:47–53
108. Meng G, Fu Q, Zha S, Xia C, Liu X, Peng D (2002) Solid State Ionics 148:533–537

109. Zhu B (2001) J Power Sources 93:82–86
110. Xia C, Li Y, Tian Y, Liu Q, Wang Z, Jia L, Zhao Y (2010) J Power Sources 195:3149–3154
111. Wang BH, Liu RQ, Wang JD, Li ZJ, Xie YH (2005) Chin J Inorg Chem 21:1551–1555
112. Wang BH, Wang JD, Liu RQ, Xie YH, Li ZJ (2007) J Solid State Electrochem 11:27–31
113. Li S, Wang X, Zhu B (2007) Electrochem Commun 9:2863–2866
114. Amar IA, Lan R, Petit CTG, Arrighi V, Tao SW (2011) Solid State Ionics 182:133–138
115. Goodenough JB (2003) Annu Rev Mater Res 33:91–128
116. Ding C, Lin H, Sato K, Hashida T (2011) Surf Coat Technol 205:2813–2817
117. Will J, Mitterdorfer A, Kleinlogel C, Perednis D, Gauckler L (2000) Solid State Ionics 131:79–96
118. Mogensen M, Sammes NM, Tompsett GA (2000) Solid State Ionics 129:63–94